

# Limitations and Accuracy of a Continuous Reduced Order Model for Modular Multilevel Converters

Andres Lopez, Daniel E. Quevedo, *Member, IEEE*, Ricardo Aguilera, *Member, IEEE*, Tobias Geyer, *Member, IEEE*, Nikolaos Oikonomou.

**Abstract**—This paper analyses the limitations of a reduced order model for Modular Multilevel Converters (MMCs) by elucidating the relation between its accuracy, operating frequency and converter parameters. A reduced order simplifies the analysis of the MMC and thereby may provide additional information about the converter behaviour. However, the accuracy of such model depends on several factors. In this paper, the effect of approximating the converter as a continuous system by neglecting quantization issues associated with having a finite number of modules is studied in detail. The analysis is done based on Fourier series approximations with which it is possible to elucidate the relationship between the resonant frequencies of the MMC and the error of the reduced order model. With the Fourier approximation, it is also possible to characterize resonant frequencies of the converter, both numerically and analytically, in terms of the converter parameters. The results can serve as a tool to identify situations when the reduced order model produces good and also less accurate approximations especially when a low number of modules are available.

## I. INTRODUCTION

Recently MMCs have become a popular power converter topology. Numerous studies have been carried out for this converter due to its advantages in high power and high voltage applications. In addition to this, its modularity, low distortion and high voltage capabilities are some other characteristics that make the MMC a very important topology for industry. Some of the industrial applications of the MMC include: wind energy conversion, HVDC grids, and medium voltage drives [1]–[3]. Due to its relevance, several studies have proposed different techniques to improve performance and address important issues. These include: modulation techniques [4]–[6], voltage balancing techniques [7], optimal capacitor ripple reduction [8], [9], several control approaches [10]–[13] and energy quality and reliability [14], [15]. All of these works also aim to understand operation principles of MMCs.

MMCs are complex power converters that exhibit a highly non-linear behaviour. In order to understand their operational principles and analyze the converter, it is important to be able to obtain relatively simple mathematical expressions that, not only describe the converter accurately, but also allow one to obtain insight into the behaviour of the system. This insight can be used as a guideline for different design purposes such

as: selection of references for control, injection of current harmonics for voltage ripple reduction or selection of control laws for different applications [16].

Several modeling approaches for the MMC have been presented in the literature. Some of these approaches are designed for simulation purposes with various levels of complexity [17]–[19]. The simpler models often neglect some of the dynamics of the converter and do not consider power losses, opening the path for more accurate methods to be proposed [20]. For a more detailed analysis of the converter a more complex model is required. In [21], [22], models that aim to obtain detailed information about the converter losses and behaviour in steady state are proposed. However, important information about the dynamics of the MMC cannot be obtained. In other works [23]–[27], more detailed continuous dynamical models of the MMC are presented. These models exhibit a reduced number of state space and control variables while maintaining the nonlinearities of the MMC. In [28], [29], these kind of models have been used to determine open-loop control strategies that use calculated steady state values and estimated voltage ripple values to achieve energy control with asymptotical stability. In general, all these models are represented in the *abc* frame, complicating the analysis of the converter due to the multiplication of two time varying signals. In [30], a more convenient representation in the *dq* frame is presented. However, the analysis is carried out for a linear case using only up to a second order harmonic.

The current manuscript extends the concept in [31] further and analyzes the impact of additional harmonic components in the converter model as well as in the control signals in more detail. This is particularly useful in the case where the number of modules are low and the quantization in the control signals is neglected in order to obtain a continuous system representation. An interesting phenomenon is that the accuracy of the model in [23] (reduced order model) is greatly affected when the operating frequency of the converter matches some specific frequencies. Following an analytical procedure, expressions for some of the frequencies where the error of the reduced order model is more significant are presented, constituting one of the main contributions of this work. These frequencies are poorly damped resonant modes that depend on the converter parameters and the harmonic content of the inputs. In [32], [33], it is shown that these poorly damped modes can generate instability in a closed loop control strategy. The method presented in this work is a straightforward alternative to identify such frequencies and therefore, it has also potential use for stability analysis [34].

Andres Lopez and Daniel E. Quevedo are with The University of Paderborn, Paderborn, Germany. e-mail: andres.lopez@upb.de, dquevedo@ieee.org.

Ricardo Aguilera is with University of Technology Sydney, Sydney, Australia. e-mail: raguilera@ieee.org.

Tobias Geyer and Nikolaos Oikonomou are with ABB Corporate Research, Baden-Dättwil, Switzerland. e-mail: {tobias.geyer, nikolaos.oikonomou}@ch.abb.com.

The current manuscript focuses on analyzing and clarifying the accuracy of the reduced order model and its relationship with the converter parameters.

The subsequent analysis shows that the accuracy of the reduced order model is low close to the resonant frequencies of the converter due to the additional frequency components introduced by quantization effects. This produces a modulation effect that displaces the resonant frequencies of the reduced order model (when continuous signals are used) in comparison with those of the full order MMC (with quantization). This generates differences in where the amplitude peak related to the resonance is located, producing inaccuracies. With sufficient knowledge about the resonant frequencies, it is possible to determine beforehand if the response of the reduced order model is accurate enough. This information can be helpful when designing an MMC based on the reduced order model. The verification of this analysis in the current manuscript is limited to a simulation environment.

This paper is organized as follows: Sections II and III present the MMC and the reduced order model respectively, Section IV discusses issues related to the application of the reduced order model. Sections V and VI estimate the resonant frequencies of the MMC using an approach based on linearization and a Fourier series expansion respectively. Finally, Section VII draws conclusions.

## II. MODULAR MULTILEVEL CONVERTER

The MMC is a power converter topology which transforms the waveform of an electrical variable from DC to AC, or vice versa (see Fig. 1) [1], [35].

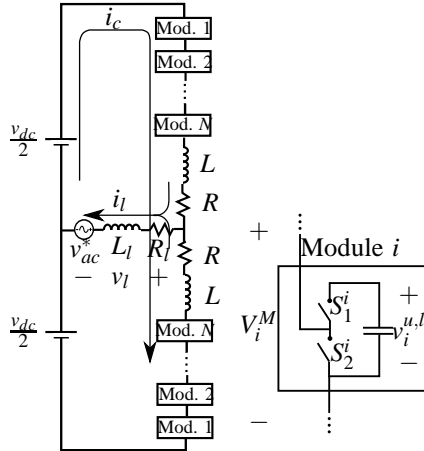


Fig. 1: MMC with  $N$  modules per arm. Here,  $v_l$  denotes the output voltage of the converter,  $i_l$  stands for the load current and  $i_c$  for the circulating current.  $S_1^i$  and  $S_2^i$  are the positions of the switches and,  $v_i^{u,l}$  and  $V_i^M$  describe the voltage of the capacitors and the modules, respectively.

In order to control the MMC, the switch positions of each module shown in Fig. 1 can be chosen independently to be one of two possible values: “inserted” or “not-inserted”. A module is considered “inserted” when its voltage ( $V_i^M$ ) is equal to the voltage of its respective capacitor. Conversely, a module is considered “not-inserted” when its voltage ( $V_i^M$ ) is equal to 0.

The desired waveforms of output currents and voltages of the MMC are sinusoidal and can be defined as

$$i_l(t) = \hat{i}_l \cos(\omega t + \phi) \quad (1)$$

$$v_l(t) = \hat{v}_l \cos(\omega t) \quad (2)$$

where  $\hat{i}_l$  is the amplitude of the output current and  $\omega$  represents the angular frequency. The phase angle  $\phi$  and the voltage amplitude  $\hat{v}_l$  can be calculated depending on  $v_{ac}^*$ ,  $R_l$  and  $L_l$ .

Using electrical circuit analysis methods, an MMC (Fig. 1) with  $N$  submodules per arm can be described by the following state space model

$$\dot{x}(t) = \mathcal{A}(\vec{\mu}^u(t), \vec{\mu}^l(t))x(t) + \mathcal{B}[v_{dc} \quad v_{ac}^*]^T \quad (3)$$

where

$$x(t) \triangleq [i_c(t) \quad i_l(t) \quad v_1^u(t) \quad \dots \quad v_N^u(t) \quad v_1^l(t) \quad \dots \quad v_N^l(t)]^T \quad (4)$$

is the system state. In (4),  $i_c$  is the circulating current, whereas  $v_i^u$  and  $v_i^l$  represent the capacitor voltages of the  $i$ -th module of the upper ( $u$ ) and lower ( $l$ ) arms. In (3),  $\vec{\mu}^u(t)$  and  $\vec{\mu}^l(t)$  represent the control signals for the modules in the upper and lower arms. Each individual component of these control signals can take the value of 1 (module inserted) or 0 (module not inserted):

$$\vec{\mu}^u(t) \triangleq [\mu_1^u(t) \quad \dots \quad \mu_N^u(t)]^T, \mu_i^u(t) \in \{0, 1\}, \quad (5)$$

$$\vec{\mu}^l(t) \triangleq [\mu_1^l(t) \quad \dots \quad \mu_N^l(t)]^T, \mu_i^l(t) \in \{0, 1\}. \quad (6)$$

The matrix  $\mathcal{A}(\vec{\mu}^u(t), \vec{\mu}^l(t))$  is defined as

$$\mathcal{A}(\vec{\mu}^u(t), \vec{\mu}^l(t)) \triangleq \begin{bmatrix} \mathcal{A}_{1,1} & \mathcal{A}_{1,2}(\vec{\mu}^u(t), \vec{\mu}^l(t)) \\ \mathcal{A}_{2,1}(\vec{\mu}^u(t), \vec{\mu}^l(t)) & 0 \end{bmatrix} \quad (7)$$

with

$$\begin{aligned} \mathcal{A}_{1,1} &= \begin{bmatrix} -\frac{R}{L} & 0 \\ 0 & -\frac{R+2R_l}{L+2L_l} \end{bmatrix} \\ \mathcal{A}_{1,2}(\vec{\mu}^u(t), \vec{\mu}^l(t)) &= \begin{bmatrix} -\frac{1}{2L}\vec{\mu}^u(t)^T & -\frac{1}{2L}\vec{\mu}^l(t)^T \\ -\frac{1}{L+2L_l}\vec{\mu}^u(t)^T & \frac{1}{L+2L_l}\vec{\mu}^l(t)^T \end{bmatrix} \\ \mathcal{A}_{2,1}(\vec{\mu}^u(t), \vec{\mu}^l(t)) &= \begin{bmatrix} \frac{1}{C}\vec{\mu}^u(t) & \frac{1}{2C}\vec{\mu}^u(t) \\ \frac{1}{C}\vec{\mu}^l(t) & -\frac{1}{2C}\vec{\mu}^l(t) \end{bmatrix} \end{aligned} \quad (8)$$

Finally,  $\mathcal{B}$  is given by:

$$\mathcal{B} \triangleq \begin{bmatrix} \frac{1}{2L} & 0 & \dots & 0 \\ 0 & -\frac{2}{L+2L_l} & \dots & 0 \end{bmatrix}^T. \quad (9)$$

## III. REDUCED ORDER MODEL AND ITS APPLICATION TO MMCs

The MMC is a discontinuous system with multiple switchable inputs as shown in (3). These discontinuities complicate the analysis of the converter. In order to simplify the analysis and obtain expressions for the variables of interest, this section investigates a model introduced and validated in [23], [36]

that reduces the order of the state space model and the number of inputs. The obtained reduced-order model is also convenient when one wishes to describe the MMC neglecting the discontinuities.

One can start defining the reduced model by considering the MMC model described in (3), and assuming that the capacitor voltages are balanced, i.e., we have:

$$v_i^u(t) = v^u(t), \quad \forall i \in \{1, 2, \dots, N\} \quad (10)$$

and<sup>1</sup>

$$v_i^l(t) = v^l(t), \quad \forall i \in \{1, 2, \dots, N\} \quad (11)$$

Then the MMC model (3) reduces to:

$$\dot{x}(t) = A \left( \check{\mu}^u(t), \check{\mu}^l(t) \right) x(t) + B [v_{dc} \quad v_{ac}^*]^T, \quad (12)$$

where

$$A \left( \check{\mu}^u(t), \check{\mu}^l(t) \right) \triangleq \begin{bmatrix} -\frac{R}{L} & 0 & -\frac{1}{2L}\check{\mu}^u(t) & -\frac{1}{2L}\check{\mu}^l(t) \\ 0 & -\frac{R+2R_l}{L+2L_l} & -\frac{1}{L+2L_l}\check{\mu}^u(t) & \frac{1}{L+2L_l}\check{\mu}^l(t) \\ \frac{1}{NC}\check{\mu}^u(t) & \frac{2}{2NC}\check{\mu}^u(t) & 0 & 0 \\ \frac{1}{NC}\check{\mu}^l(t) & -\frac{1}{2NC}\check{\mu}^l(t) & 0 & 0 \end{bmatrix} \quad (13)$$

$$B \triangleq \begin{bmatrix} \frac{1}{2L} & 0 & 0 & 0 \\ 0 & -\frac{2}{L+2L_l} & 0 & 0 \end{bmatrix}^T \quad (14)$$

and the system state is now given by

$$x(t) \triangleq [i_c(t) \quad i_l(t) \quad v^u(t) \quad v^l(t)]^T. \quad (15)$$

In this model, the modulation functions are

$$\check{\mu}^u(t) \triangleq \sum_{j=1}^N \mu_j^u(t), \quad \check{\mu}^u(t) \in \{0, \dots, N\} \quad (16)$$

and

$$\check{\mu}^l(t) \triangleq \sum_{j=1}^N \mu_j^l(t), \quad \check{\mu}^l(t) \in \{0, \dots, N\} \quad (17)$$

These functions represent the number of modules inserted in the upper and lower arms respectively, and depend on the control law adopted.

A detailed procedure to obtain the previous expressions can be found in [23].

As stated before, the reduced-order model in (12) uses the control signals in (16) and (17). Since these aggregated control signals are the sum of the binary control signals  $\mu_j^{u,l}$ , they represent quantized signals that only take integer values between 0 and  $N$ .

The reduced order model facilitates the derivation of analytical solutions by reducing the number of input variables and the size of the state vector. This can be used for a more detailed analysis of the converter such as in [23], [36].

It is important to note that when the reduced order model is used, it is implicitly assumed that the voltages in all the capacitors are balanced according to Eqs. (10) and (11). Note that when this condition is fulfilled, it is possible to

represent the capacitors of all modules with one capacitor per arm and define aggregated control signals  $\mu_j^{u,l}$  without using any approximation. All the information about any modulation technique used, or about the control inputs  $\mu_j^{u,l}$  in general, is now contained in  $\check{\mu}^{u,l}$  as defined in Eqs. (16) and (17). Thus, if the voltages of the capacitors are balanced (see Eqs. (10) and (11)), then the full order model and the reduced order model using  $\check{\mu}^{u,l}$  provide the same result.

#### IV. IMPLICATIONS OF USING THE REDUCED ORDER MODEL

##### A. Using continuous control signals

In some cases, it may be convenient to express the aggregated control signals in Eqs. (16) and (17) as the sum of an equivalent continuous valued signal  $\mu^{u,l}(t)$  and a quantization effect  $Q_n(t)$ , produced by having only a finite number of modules in the converter, as follows:

$$\check{\mu}^{u,l}(t) = \mu^{u,l}(t) + Q_n(t). \quad (18)$$

If desired,  $Q_n(t)$  can be neglected using only the continuous part  $\mu^{u,l}(t)$ . In particular, if  $\mu^{u,l}(t)$  are smooth, then only differentiable functions need to be taken into account, easing the analysis. Note that this step implies an approximation and it is specially important when a low number of modules are available ( $Q_n(t)$  comparable with  $\mu^{u,l}(t)$ ). It is because of this approximation that the results of the reduced order model may differ from the ones of the full order MMC.

Neglecting the quantization allows one to obtain analytical expressions of variables such as the capacitor voltages. These expressions can then be used for optimization and reference design [23]. However, the quantization affects the frequency response of the circuit, leading to inaccuracies when this is neglected.

Due to the non-linearity in the model, there is a modulation effect that comes from the multiplication of the control signal with the capacitor voltages, see Eq. (12). This effect moves the resonant frequencies (i.e. peaks of amplitude in  $i_c$ ) of the converter when additional frequency components are considered in the control signals. As shown next, this accentuates the error of the reduced order model at some specific frequencies.

To illustrate the effect of the quantization at different frequencies, let us consider numerical values of the parameters of the converter as in Table I. Moreover, let us define the following control inputs:

- smooth control inputs:

$$\mu^u(t) = N \frac{1 + \cos(\omega t)}{2}, \quad \mu^l(t) = N \frac{1 - \cos(\omega t)}{2}. \quad (19)$$

- quantized control inputs:

$$\check{\mu}^u(t) = ni \left( N \frac{1 + \cos(\omega t)}{2} \right), \quad \check{\mu}^l(t) = ni \left( N \frac{1 - \cos(\omega t)}{2} \right), \quad (20)$$

where the operation  $ni(\bullet)$  approximates the argument to the nearest integer.

Fig. 2 shows the response of an open loop MMC to the control inputs in Eqs. (19) and (20) with fundamental frequency  $\omega = 2\pi 60$ . A clear difference between the two cases

<sup>1</sup>Note that  $v^u(t) = v^l(t)$  is not imposed. Thus the model allows capacitor voltages in the upper to be different from those in the lower arm.

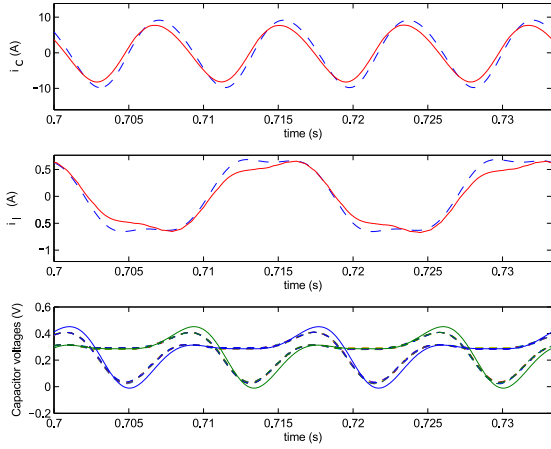


Fig. 2: Effects of the quantization at  $60\text{Hz}$  (Solid lines: without quantization, dashed lines: with quantization)

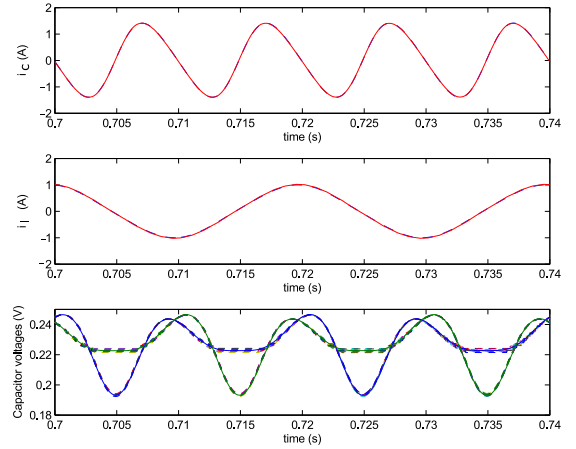


Fig. 3: Effects of the quantization at  $50\text{Hz}$  (Solid lines: without quantization, dashed lines: with quantization)

(with and without quantization) can be observed. Interestingly, the situation changes when the frequency of the sinusoidal input is changed to  $\omega = 2\pi 50$ , see Fig. 3. The simulation shows that the difference between the response of the model without the quantization and the model with the quantization is minimal for this frequency. In Fig. 4, a simulation with the error produced by neglecting the quantization effect for MMCs with different number of modules is shown. The error is calculated as the Root Mean Square of the difference of the simulated waveforms over one period in steady state. The simulation shows that a larger error is presented for some specific frequencies. We shall give special attention to the peak with the highest frequency since it may be located close to the typical operating frequencies of the converter ( $50\text{Hz}$  or  $60\text{Hz}$ ). This observation shows that the quality of the model is frequency dependent and motivates our subsequent analysis.

Let us first define what we shall refer to as the “frequency response of the MMC”. Due to the non-linear nature of the system, frequencies multiples of the input frequency are likely to appear in the converter currents and voltages. This motivates us to define the frequency response of the MMC as the amplitude of the second harmonic of the circulating current  $i_c$  as a function of the frequency in the control signals  $\omega$  (see Eqs. (19) and (20)). The reason why the second harmonic of  $i_c$  is chosen for the analysis is mainly due to the following facts: (i) this is the lowest order harmonic in the circulating current, (ii) its amplitude is significantly higher than the amplitude of the other harmonics, (iii) as shown in Fig. 4, the resonance of this second order harmonic is more likely to match the operating frequency of the converter<sup>2</sup>. In the following sections we are going to focus our efforts into determining the relation of these resonant frequencies with the converter parameters.

<sup>2</sup>Note that the resonant frequencies are independent of our choice of considering the second order harmonic of  $i_c$  as output variable for the analysis.

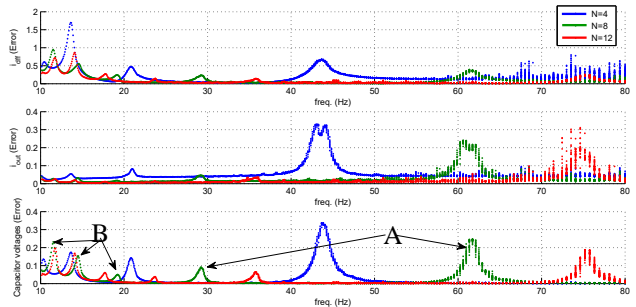


Fig. 4: Error produced by the quantization effect using 4, 8 and 12 modules for different frequency values. (A) High frequency peaks. (B) Low frequency peaks.

TABLE I: Parameter values in p.u. at  $\omega = 2\pi 50$  for an MMC (The p.u. (per unit) values are normalized with respect to the grid voltage (3800 V) and the nominal current (650 A))

| Variable | $R$   | $X_L (\omega L)$ | $X_C (\frac{1}{\omega C})$ | $R_l$ | $X_{L_l} (\omega L_l)$ | $v_{dc}$ | $v_{ac}^*$ | $N$ |
|----------|-------|------------------|----------------------------|-------|------------------------|----------|------------|-----|
| Value    | 0.004 | 0.075            | 0.089                      | 0.01  | 0.15                   | 2.19     | 1          | 8   |

### B. Effects of capacitor voltage imbalances

Test have shown that the error in the converter currents (i.e.  $i_c$  and  $i_l$ ) of the reduced order model, when compared with the full order model, presents an increment of less than 10%, with an allowed voltage imbalance of up to 35% of the module voltage ripple (voltage ripple measured in balanced condition). It is worth noticing that the circulating current is more affected by the voltage imbalances due to the low arm impedance.

## V. ESTIMATION OF THE MMC RESONANT FREQUENCIES (LINEARIZATION APPROACH)

This section presents a preliminary approach to obtain information about the frequency response of the MMC that uses a linearized version of the reduced order model around an operation point. The linearization technique is widely used in many applications. One of them is design of control laws for power converters, where it is important that the information provided by the linearized model matches as close as possible the original model to guarantee proper performance and good

stability properties. This approach aims to derive simple analytical expressions for the resonant frequencies based on linear differential equations that later will be used for comparison with more elaborated approaches. This will also serve as a criteria to determine the accuracy of the linearized model of the MMC.

The linear model can be written, based in Eq. (12), as follows:

$$\dot{\tilde{x}}(t) = A(\bar{\mu}^u, \bar{\mu}^l) \tilde{x}(t) + B(x(0)) [v_{dc} \quad v_{ac}^* \quad \tilde{\mu}^{u,l}(t)]^T, \quad (21)$$

where  $\bar{\mu}^{u,l}$  represent the control signals in the operational point,  $\tilde{\mu}^{u,l}(t)$  and  $\tilde{x}(t) = [\tilde{i}_c \quad \tilde{i}_l \quad \tilde{v}^u \quad \tilde{v}^l]$  the incremental variables associated with the control signals and the state space vector respectively, and  $B(x(0))$  a constant matrix that depends on the initial conditions  $x(0)$ . Since the matrix  $A(\bar{\mu}^u, \bar{\mu}^l)$  is in charge of determine the placement of the poles and resonant frequencies of the system, we focus our analysis in this term of the equation.

To simplify the calculations, let us assume that  $\|R + j\omega L\| \ll \|R_l + j\omega L_l\|$ . Therefore, the resonant frequencies can be analyzed by considering two different cases; a case for the higher frequencies and an additional case for the lower frequencies

The following analysis uses this assumption and the linearized model in Eq. (21) to derive analytical expressions of the resonant frequencies of the MMC. In Section VI, the results of the resonant frequencies obtained with the linearized model will be compared with results obtained with more accurate methods, which can be very useful when one wish to evaluate the accuracy of the linearized model specially in the case of stability of control loops. Moreover, it will provide more insight into the problem explaining the results in Fig. 4.

### A. High Frequencies

Under the assumptions  $\|R + j\omega L\| \ll \|R_l + j\omega L_l\|$ , it is possible to write the differential equations of the linear system in Eq. (21) and, taking into account that the operation lies in the high frequency range (i.e.  $\|R_l + j\omega L_l\| \rightarrow \infty$  or  $i_l = 0$ ), develop analytical expressions for the resonant frequencies of the converter. According to Eq. (21) and considering that  $\bar{\mu}^u + \bar{\mu}^l = N$  and  $\bar{\mu}^u = \alpha N$ , where  $0 < \alpha < 1$  is a constant value that depends on the linearization point, a value for the resonant frequency can be obtained as:

$$f_1 = \frac{1}{\sqrt{\frac{2LC}{N} \frac{1}{\alpha^2 + (1-\alpha)^2}}}, \quad \frac{\sqrt{2}}{2} \frac{1}{\sqrt{\frac{2LC}{N}}} \leq f_1 < \frac{1}{\sqrt{\frac{2LC}{N}}} \quad (22)$$

Due to the fact that  $i_c$  contains mainly second order harmonics, an interesting phenomenon occurs. This consists in the resonance being produced when the input frequency is equals to  $\frac{f_1}{2}$ . Due to the system non-linearities, this input frequency produces an  $i_c$  with frequency  $f_1$ , matching the resonance frequency. Note that this phenomenon is not captured by the linear model analyzed in this section. This will be corroborated and analysed further with the method presented in Section VI.

### B. Low Frequencies

For the low frequency case,  $R$  and  $L$  are considered as 0. Eq. (21) can be used under this consideration to obtain a resonant frequency as:

$$f_2 = \frac{1}{\sqrt{\frac{L_l C}{N} \left( \frac{\alpha^2 + (1-\alpha)^2}{\alpha^2 (1-\alpha)^2} \right)}}, \quad 0 < f_2 \leq \frac{\sqrt{2}}{4} \frac{1}{\sqrt{\frac{L_l C}{N}}} \quad (23)$$

## VI. ESTIMATION OF THE MMC RESONANT FREQUENCIES (FOURIER APPROACH)

In order to address the problem of obtaining information about the frequency response of the MMC in more detail, an approach using Fourier series approximation that analyzes each frequency component separately is applied. For detailed information of such techniques please refer to [37], [38]. In [39], [40], this Fourier method is applied to an MMC under nominal operating conditions and validated against a fully detailed electromagnetic transient model in PSCAD/EMTDC [41].

The results in [39], [40] show good accuracy of the Fourier series approximation with as low as 2 harmonic components. Moreover, it is also shown that, by increasing the harmonic components up to 17, the results are considerably improved, obtaining a very close match between the model in PSCAD/EMTDC and the approach using Fourier series. Therefore, we shall consider the model presented in this section can be considered as a good reference for the accuracy assessment of the reduced order model.

Using the Fourier series approximation, the MMC can be described by the following equation

$$\mathbf{M}(\omega)\mathbf{z} = \mathbf{U} \quad (24)$$

where

$$\mathbf{M}(\omega) \triangleq \begin{bmatrix} -(R\mathbf{I} + j\omega N L) & 0 & -\frac{1}{2}\mathbf{Y}_u & -\frac{1}{2}\mathbf{Y}_l \\ 0 & -(\frac{R+2R_l}{L+2L_l}\mathbf{I} + j\omega N L_l) & -\frac{L_l}{L+2L_l}\mathbf{Y}_u & \frac{1}{L+2L_l}\mathbf{Y}_l \\ \frac{1}{N C}\mathbf{Y}_u & \frac{1}{2N C}\mathbf{Y}_u & -j\omega N C & 0 \\ \frac{1}{N C}\mathbf{Y}_l & -\frac{1}{2N C}\mathbf{Y}_l & 0 & -j\omega N C \end{bmatrix} \quad (25)$$

$$\mathbf{U} \triangleq \begin{bmatrix} -\frac{1}{2}\mathbf{V}_{in} & 0 & 0 & 0 \\ 0 & \frac{2L_l}{L+2L_l}\mathbf{V}_{ac}^* & 0 & 0 \end{bmatrix}^T \quad (26)$$

and

$$\mathbf{z} \triangleq [\mathbf{I}_c \quad \mathbf{I}_l \quad \mathbf{V}^u \quad \mathbf{V}^l]^T \quad (27)$$

are matrices constructed based on the Fourier transformation of Eq. (12). The diagonal matrix  $\mathbf{n}$  is defined as follows

$$\mathbf{n} \triangleq \text{diag}([-n \quad -(n-1) \quad \dots \quad 0 \quad \dots \quad n-1 \quad n]) \quad (28)$$

where  $n$  is the number of frequency components used in the Fourier series expansion.

The variables  $\mathbf{V}_{in}$ ,  $\mathbf{V}_{ac}^*$ ,  $\mathbf{I}_c$ ,  $\mathbf{I}_l$ ,  $\mathbf{V}^u$  and  $\mathbf{V}^l$  are vectors that contain each of the coefficients of the Fourier series expansion

of the respective variable. As an example, let us assume that  $i_c(t)$  can be written as:

$$i_c(t) = \sum_{k=-n}^n i_c^{(k)} e^{j\omega t}. \quad (29)$$

With this, the variable  $\mathbf{I}_c$  can be defined as follows

$$\mathbf{I}_c \triangleq \begin{bmatrix} i_c^{(-n)} & \dots & i_c^{(0)} & \dots & i_c^{(n)} \end{bmatrix}^T. \quad (30)$$

where  $i_c^{(j)}$  represent the coefficient corresponding to the  $j^{\text{th}}$  multiple of the natural frequency of  $i_c$ .

The matrices  $\mathbf{Y}_j$  represent the Fourier decomposition of the control inputs and are defined as follows:

$$\mathbf{Y}_j \triangleq \begin{bmatrix} Y_j^{(0)} & \dots & Y_j^{(-2n)} \\ \vdots & \ddots & \vdots \\ Y_j^{(2n)} & \dots & Y_j^{(0)} \end{bmatrix} \quad (31)$$

where  $Y_j^{(k)}$  represent the coefficient corresponding to the  $k^{\text{th}}$  multiple of the natural frequency of the control signals  $\mu^j$ .

With the previous definitions, the vector  $\mathbf{z}$  can be found using the following expression (see Eq. (24))

$$\mathbf{z} = (\mathbf{M}(\omega))^{-1} \mathbf{U}. \quad (32)$$

Since the system described by Eq. (24) is linear, it is possible to find the resonant frequencies of the system by solving for  $\omega$  the following equation

$$\det(\mathbf{M}(\omega)) = 0 \quad (33)$$

In order to illustrate the results of this method, Fig. 5 shows the frequency response of  $i_c$  for different numbers of frequency components  $n$ . It can be seen that the resonant frequencies move and some new ones appear when the value of  $n$  is increased. In particular, the peaks marked as "A" correspond to the resonance of the 2nd harmonic of  $i_c$ , "B" to the resonance of the 4th harmonic, "C" to the resonance of the 6th harmonic. The peaks marked as "D" correspond to the resonances dominated by the load impedance.

It is possible to obtain analytical expressions for some of the resonant frequencies in terms of the converter components. This can be done by solving (33) for a given value of  $n$ . For the sake of simplicity, only the continuous control signals in Eq. (19) are going to be considered for this analysis.

Note that the frequency response may change, if the amplitude or characteristics of these control signals change due to the nonlinear properties of the system.

The results of the analysis of the frequency response using the Fourier series are shown in the sections below. For some numerical comparisons, the values of Table I are used

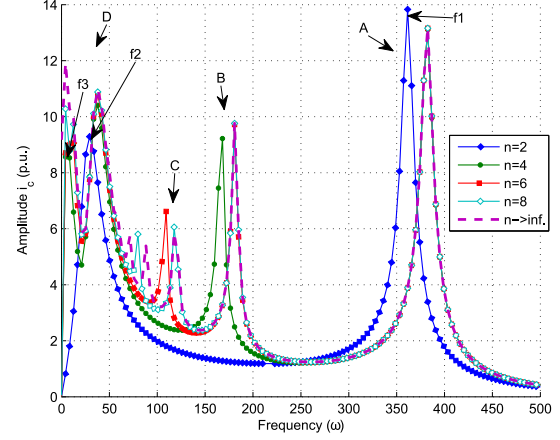


Fig. 5: Estimation of the amplitude of  $i_c$  using the Fourier series approximation for different values of  $n$

#### A. Frequency response analysis with $n = 2$

In order to begin with the analysis, matrices  $\mathbf{n}$ ,  $\mathbf{Y}_u$ ,  $\mathbf{Y}_1$  and  $\mathbf{U}$  in Eqs. (14), (28) and (31) respectively, need to be defined using  $n = 2$  and the control signals in Eq. (19). These matrices can be used to define  $M(\omega)$  (see Eq. (25)) and then to obtain the solution  $\mathbf{z}$  by applying Eq. (32). Consequently, the resonant frequencies can be obtained using Eq. (33).

After some algebraic manipulations, the following simplified expressions for the frequencies  $f_1$  and  $f_2$  in Fig. 5 can be derived

$$f_1 = \left( \frac{16CLL_1R^2 + 16CL_1^2R^2 - 8L^3N - 22L^2L_1N - 12LL_1^2N}{32CL^2(L^2 + 4LL_1 + 4L_1^2)} - \frac{28CL^2R^2 + 80CL^2RR_1 + 64CL^2R_1^2}{32CL^2(L^2 + 4LL_1 + 4L_1^2)} \right)^{\frac{1}{2}}, \quad (34)$$

$$f_2 = \text{Re} \left( \sqrt{\frac{L_1N - 32CR_1^2 + 8\sqrt{16C^2R_1^4 - CL_1NR_1^2}}{64L_1^2C}} \right). \quad (35)$$

where  $\text{Re}(\ast)$  represents the real part of the argument. Table II shows a comparison of the numerical values of the resonant frequencies obtained with different methods. It can be seen that the analytical expressions (Eqs. (34) and (35)) approximate the numerical results with an error less than 4%. The approach based on linearization in Section V gives a very easy method to compute these values, however the accuracy of the result is compromised. Note that the phenomenon mentioned in Section V where the resonance due to  $f_1$  is produced when the input is at  $\frac{f_1}{2}$  can be seen clearly in this comparison. The linearized approach fails to model this phenomenon producing values for  $f_1$  that are around twice as high as the actual value. Remember also that  $f_1$  is of special importance since it could match the operating frequency of the converter and thereby producing inaccuracies in the reduced order model.

TABLE II: Comparison of the resonant frequencies  $f_1$  and  $f_2$  (see Fig. 5) obtained with different methods for  $n = 2$ : Actual: Using Eq. (33) with  $n \rightarrow \infty$  and quantized control signals. Fourier (Num.): Using Eq. (33) with  $n = 2$  and continuous control signals. Fourier (Ana.): Using Eqs. (34) and (35). Lin.: Using Eqs. (22) and (23)

|       | Actual | Fourier (Num.) | Fourier (Ana.) | Lin.          |
|-------|--------|----------------|----------------|---------------|
| $f_1$ | 382.6  | 361.4          | 362.4          | 582.4 - 823.7 |
| $f_2$ | 50.4   | 29.3           | 28.3           | 0 - 265.5     |

### B. Frequency response analysis with $n \geq 4$

The complexity of the expressions obtained by solving (32) grows exponentially with  $n$ . For  $n = 4$  it is possible to obtain relatively simple analytical expressions only for some low importance frequencies. Therefore, beyond this point, it is necessarily to proceed with numerical solutions.

### C. Effects of the quantization $Q_n(t)$ of the control signals

Due to the non-linear nature of the system, the inclusion of the quantization change the frequency response of the system. To take this effect into account, the control signals in Eq. (20) are used for the following analysis.

Fig. 6 shows a comparison of the frequency response of the reduced order model calculated with the Fourier approximation for  $n = 2$  with and without the quantization. It can be seen how the resonant frequencies change their position and the amplitudes of the peaks are slightly attenuated. Unfortunately, it is not possible to obtain analytical expression for the resonant frequencies when the quantization is taken into account for  $n \geq 2$  due to the complexity of the expressions. However, they can be obtained numerically by solving Eq. (33).

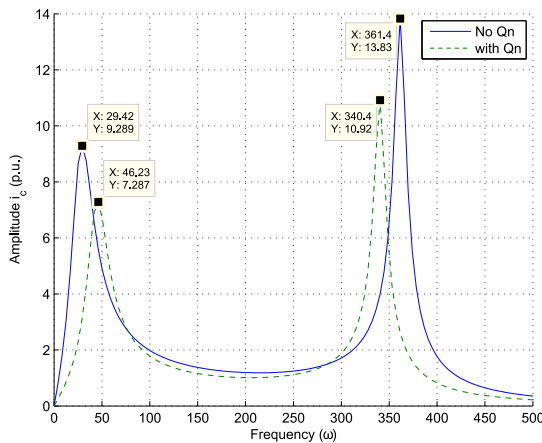


Fig. 6: Frequency response of the MMC for  $n = 2$  with and without quantization

Fig. 7 shows the results for  $n = 6$ . For this case, the resonant frequencies are also affected by the quantization; especially, the amplitude corresponding to the resonance of the 4<sup>th</sup> harmonic (frequency peak between 150 rad/s and 200 rad/s) is attenuated significantly once the quantization is taken into account. Moreover, the resonant frequency with the highest value is displaced around 7% due to the quantization. This

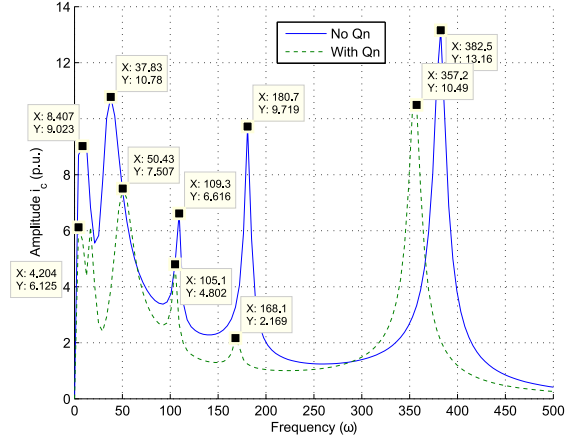


Fig. 7: Frequency response of the MMC for  $n = 6$  with and without quantization

displacement in frequency is less pronounced for the other resonant frequencies.

The difference of the two frequency responses in Fig. 7 corresponds to the error caused by neglecting the quantization. Since the amplitude peaks are at slightly different locations, the difference between the two frequency responses become significant close to them. This explains the peaks obtained in the simulation already shown in Fig. 4, where the error of the model without quantization was illustrated.

## VII. CONCLUSIONS

A reduced order model can accurately represent the behaviour of the MMC in many situations. However, aspects as voltage imbalances and quantization can affect its accuracy. This work analyses the impact of both of these aspects on the accuracy of the reduced order model showing how voltage imbalances affect the model error. Moreover, the effect of the quantization in the control signals for different operation frequencies is also addressed. The current manuscript has extensively analyzed the inaccuracy introduced by the quantization effect as a function of the frequency of operation showing that, in frequency ranges close to the resonant frequencies, the accuracy of the reduced order model is reduced.

This work has developed detailed methods to characterize resonant frequencies of MMC's by using analytical expressions. This novel analysis allows one to obtain values of the resonant frequencies that have not been identified in the current literature, giving additional insight on the MMC. The results obtained here can be used to estimate beforehand if the reduced order model produces an accurate representation of the MMC, and the insight gained is particularly useful when working with control techniques using continuous control signals.

## REFERENCES

- [1] A. Lesnicar and R. Marquardt, "An innovative modular multilevel converter topology suitable for a wide power range," in *Power Tech Conference Proceedings, 2003 IEEE Bologna*, vol. 3, June 2003, pp. 6 pp. Vol.3-.

- [2] M. Malinowski, K. Gopakumar, J. Rodriguez, and M. Perez, "A survey on cascaded multilevel inverters," *Industrial Electronics, IEEE Transactions on*, vol. 57, no. 7, pp. 2197–2206, July 2010.
- [3] M. Perez, S. Bernet, J. Rodriguez, S. Kouro, and R. Lizana, "Circuit topologies, modeling, control schemes, and applications of modular multilevel converters," *Power Electronics, IEEE Transactions on*, vol. 30, no. 1, pp. 4–17, Jan 2015.
- [4] K. Ilves, A. Antonopoulos, S. Norrga, and H.-P. Nee, "A new modulation method for the modular multilevel converter allowing fundamental switching frequency," *Power Electronics, IEEE Transactions on*, vol. 27, no. 8, pp. 3482–3494, 2012.
- [5] M. Huang, J. Zou, and X. Ma, "An improved phase-shifted carrier modulation for modular multilevel converter to suppress the influence of fluctuation of capacitor voltage," *IEEE Transactions on Power Electronics*, vol. 31, no. 10, pp. 7404–7416, Oct. 2016.
- [6] S. Lu, L. Yuan, K. Li, and Z. Zhao, "An improved phase-shifted carrier modulation scheme for hybrid modular multilevel converter," *IEEE Transactions on Power Electronics*, vol. PP, no. 99, p. 1, 2016.
- [7] S. Fan, K. Zhang, J. Xiong, and Y. Xue, "An improved control system for modular multilevel converters with new modulation strategy and voltage balancing control," *Power Electronics, IEEE Transactions on*, vol. 30, no. 1, pp. 358–371, Jan 2015.
- [8] K. Ilves, A. Antonopoulos, L. Harnefors, S. Norrga, L. Angquist, and H.-P. Nee, "Capacitor voltage ripple shaping in modular multilevel converters allowing for operating region extension," in *IECON 2011-37th Annual Conference on IEEE Industrial Electronics Society*. IEEE, 2011, pp. 4403–4408.
- [9] R. Picas, J. Pou, S. Ceballos, J. Zaragoza, G. Konstantinou, and V. Agelidis, "Optimal injection of harmonics in circulating currents of modular multilevel converters for capacitor voltage ripple minimization," in *ECCE Asia Downunder*, June 2013, pp. 318–324.
- [10] J. Qin and M. Saedifard, "Predictive control of a modular multilevel converter for a back-to-back HVDC system," *IEEE Transactions on Power Delivery*, vol. 27, no. 3, pp. 1538–1547, 2012.
- [11] B. Riar, T. Geyer, and U. Madawala, "Model predictive direct current control of modular multilevel converters: Modeling, analysis, and experimental evaluation," *Power Electronics, IEEE Transactions on*, vol. 30, no. 1, pp. 431–439, Jan 2015.
- [12] M. Perez, J. Rodriguez, E. Fuentes, and F. Kammerer, "Predictive control of ac-ac modular multilevel converters," *Industrial Electronics, IEEE Transactions on*, vol. 59, no. 7, pp. 2832–2839, July 2012.
- [13] Z. Gong, P. Dai, X. Yuan, X. Wu, and G. Guo, "Design and experimental evaluation of fast model predictive control for modular multilevel converters," *IEEE Transactions on Industrial Electronics*, vol. 63, no. 6, pp. 3845–3856, Jun. 2016.
- [14] J. Xu, P. Zhao, and C. Zhao, "Reliability analysis and redundancy configuration of mmc with hybrid submodule topologies," *IEEE Transactions on Power Electronics*, vol. 31, no. 4, pp. 2720–2729, Apr. 2016.
- [15] D. Wu and L. Peng, "Analysis and suppressing method for the output voltage harmonics of modular multilevel converter," *IEEE Transactions on Power Electronics*, vol. 31, no. 7, pp. 4755–4765, Jul. 2016.
- [16] K. Sharifabadi, L. Harnefors, H.-P. Nee, R. Teodorescu, and S. Norrga, *Design, Control and Application of Modular Multilevel Converters for HVDC Transmission Systems*. John Wiley & Sons, 2016.
- [17] J. Peralta, H. Saad, S. Denetiere, J. Mahseredjian, and S. Nguefeu, "Detailed and averaged models for a 401-level mmc –HVDC system," *IEEE Transactions on Power Delivery*, vol. 27, no. 3, pp. 1501–1508, Jul. 2012.
- [18] J. Xu, A. M. Gole, and C. Zhao, "The use of averaged-value model of modular multilevel converter in DC grid," *IEEE Transactions on Power Delivery*, vol. 30, no. 2, pp. 519–528, Apr. 2015.
- [19] U. Gnanarathna, A. Gole, and R. Jayasinghe, "Efficient modeling of modular multilevel hvdc converters (mmc) on electromagnetic transient simulation programs," *Power Delivery, IEEE Transactions on*, vol. 26, no. 1, pp. 316–324, 2011.
- [20] A. Beddard, C. Sheridan, M. Barnes, and T. Green, "Improved accuracy average value models of modular multilevel converters," *IEEE Transactions on Power Delivery*, vol. PP, no. 99, p. 1, 2016.
- [21] S. Rodrigues, A. Papadopoulos, E. Kontos, T. Todorovic, and P. Bauer, "Steady-state loss model of half-bridge modular multilevel converters," *IEEE Transactions on Industry Applications*, vol. 52, no. 3, pp. 2415–2425, May 2016.
- [22] Q. Song, W. Liu, X. Li, H. Rao, S. Xu, and L. Li, "A steady-state analysis method for a modular multilevel converter," *IEEE Transactions on Power Electronics*, vol. 28, no. 8, pp. 3702–3713, Aug. 2013.
- [23] A. Lopez, D. E. Quevedo, R. P. Aguilera, T. Geyer, and N. Oikonomou, "Reference design for predictive control of modular multilevel converters," in *Australian Control Conference (AUCC)*, 2014.
- [24] S. Rohner, J. Weber, and S. Bernet, "Continuous model of modular multilevel converter with experimental verification," in *Energy Conversion Congress and Exposition (ECCE), 2011 IEEE*, 2011, pp. 4021–4028.
- [25] N. Ahmed, L. Angquist, S. Norrga, A. Antonopoulos, L. Harnefors, and H.-P. Nee, "A computationally efficient continuous model for the modular multilevel converter," *Emerging and Selected Topics in Power Electronics, IEEE Journal of*, vol. 2, no. 4, pp. 1139–1148, Dec 2014.
- [26] H. Yang, Y. Dong, W. LI, and X. HE, "Average-value model of modular multilevel converters considering capacitor voltage ripple," *IEEE Transactions on Power Delivery*, vol. PP, no. 99, p. 1, 2016.
- [27] L. Harnefors, A. Antonopoulos, S. Norrga, L. Angquist, and H.-P. Nee, "Dynamic analysis of modular multilevel converters," *IEEE Transactions on Industrial Electronics*, vol. 60, no. 7, pp. 2526–2537, 2013.
- [28] L. Angquist, A. Antonopoulos, D. Siemaszko, K. Ilves, M. Vasiladiotis, and H.-P. Nee, "Open-loop control of modular multilevel converters using estimation of stored energy," *IEEE transactions on industry applications*, vol. 47, no. 6, pp. 2516–2524, 2011.
- [29] A. Antonopoulos, L. Ängquist, L. Harnefors, K. Ilves, and H.-P. Nee, "Global asymptotic stability of modular multilevel converters," *IEEE Transactions on Industrial Electronics*, vol. 61, no. 2, pp. 603–612, 2014.
- [30] A. Jamshidifar and D. Jovic, "Small-signal dynamic dq model of modular multilevel converter for system studies," *IEEE Transactions on Power Delivery*, vol. 31, no. 1, pp. 191–199, Feb. 2016.
- [31] K. Ilves, A. Antonopoulos, S. Norrga, and H.-P. Nee, "Steady-state analysis of interaction between harmonic components of arm and line quantities of modular multilevel converters," *IEEE transactions on power electronics*, vol. 27, no. 1, pp. 57–68, 2012.
- [32] T. LI, A. M. Gole, and C. Zhao, "Harmonic instability in mmc-HVDC converters resulting from internal dynamics," *IEEE Transactions on Power Delivery*, vol. PP, no. 99, p. 1, 2016.
- [33] J. Lyu, X. Cai, and M. Molinas, "Frequency domain stability analysis of mmc-based hvdc for wind farm integration," *IEEE Journal of Emerging and Selected Topics in Power Electronics*, vol. 4, no. 1, pp. 141–151, Mar. 2016.
- [34] N. R. Chaudhuri, R. Oliveira, and A. Yazdani, "Stability analysis of vector-controlled modular multilevel converters in linear time-periodic framework," *IEEE Transactions on Power Electronics*, vol. 31, no. 7, pp. 5255–5269, Jul. 2016.
- [35] R. Marquardt, "Modular multilevel converter: An universal concept for hvdc-networks and extended dc-bus-applications," in *Power Electronics Conference (IPEC), 2010 International*, June 2010, pp. 502–507.
- [36] A. Lopez, D. E. Quevedo, R. P. Aguilera, T. Geyer, and N. Oikonomou, "Validation of a reduced order model for modular multilevel converters and analysis of circulating current," in *EPE15 ECCE Europe*, 2015.
- [37] R. Trincherro, I. Stievano, and F. Canavero, "Steady-state analysis of switching power converters via augmented time-invariant equivalents," *Power Electronics, IEEE Transactions on*, vol. 29, no. 11, pp. 5657–5661, Nov 2014.
- [38] S. Norrga, L. Angquist, K. Ilves, L. Harnefors, and H. Nee, "Frequency-domain modeling of modular multilevel converters," in *IECON 2012 - 38th Annual Conference on IEEE Industrial Electronics Society*, Oct 2012, pp. 4967–4972.
- [39] D. Jovic and A. A. Jamshidifar, "Phasor model of modular multilevel converter with circulating current suppression control," *IEEE Transactions on Power Delivery*, vol. 30, no. 4, pp. 1889–1897, 2015.
- [40] S. Rajesvaran and S. Filizadeh, "Modeling modular multilevel converters using extended-frequency dynamic phasors," in *Power and Energy Society General Meeting (PESGM), 2016*. IEEE, 2016, pp. 1–5.
- [41] J. Peralta, H. Saad, S. Denetiere, J. Mahseredjian, and S. Nguefeu, "Detailed and averaged models for a 401-level mmc–hvdc system," *IEEE Transactions on Power Delivery*, vol. 27, no. 3, pp. 1501–1508, 2012.